

## Graphitized carbon on GaAs(100) substrates

J. Simon,<sup>1,a)</sup> P. J. Simmonds,<sup>1</sup> J. M. Woodall,<sup>2</sup> and M. L. Lee<sup>1</sup>

<sup>1</sup>Department of Electrical Engineering, School of Engineering and Applied Science, Yale University, New Haven, Connecticut 06520-8284, USA

<sup>2</sup>School of Electrical and Computer Engineering, Purdue University, West Lafayette, Indiana 47907-2035, USA

(Received 28 December 2010; accepted 27 January 2011; published online 18 February 2011)

We report on the formation of graphitized carbon on GaAs(100) surfaces by molecular beam epitaxy. We grew highly carbon-doped GaAs on AlAs, which was then thermally etched *in situ* leaving behind carbon atoms on the surface. After thermal etching, Raman spectra revealed characteristic phonon modes for  $sp^2$ -bonded carbon, consistent with the formation of graphitic crystallites. We estimate that the graphitic crystallites are 1.5–3 nm in size and demonstrate that crystallite domain size can be increased through the use of higher etch temperatures. © 2011 American Institute of Physics. [doi:10.1063/1.3555442]

Graphene has gained significant attention recently due to its ultrahigh mobility,<sup>1</sup> conical band structure,<sup>2</sup> and tunable band gap by the use of nanoribbons.<sup>3</sup> This allows for its use in a variety of applications, including field effect<sup>4</sup> and tunneling<sup>5</sup> transistors, electronic interconnects,<sup>6</sup> and transparent contacts.<sup>7</sup> Since the first isolation of graphene<sup>2</sup> there has been increasing interest in developing large scale graphene sheets for electronic devices. Currently, epitaxial graphene sheets are grown either by chemical vapor deposition (CVD) on metal films<sup>8,9</sup> or by the graphitization of SiC substrate surfaces by sublimation of Si atoms at high temperatures.<sup>10,11</sup> The CVD approach allows for close control of the number of graphene sheets formed.<sup>8</sup> However, graphene domain size is limited by the distance between the metal grain boundaries.<sup>8</sup> Furthermore, CVD-grown graphene needs to be transferred to a separate carrier wafer for device fabrication.<sup>9</sup> In contrast, graphene devices can be fabricated directly on insulating SiC wafers.<sup>12,13</sup> However, graphene epitaxy on SiC is still constrained by the high substrate cost, poor control of number of graphene layers, and rough substrate surfaces.<sup>14</sup> These limitations have led to the continued search for a more effective way to grow graphene sheets for large scale device processing. In this letter we report on the graphitization of GaAs(100) surfaces by molecular beam epitaxy (MBE) and

propose it as a future alternative for the production of large scale graphene sheets.

MBE-based carbon deposition techniques for graphitizing various substrates have been developed recently. Garcia *et al.* developed an approach in which they deposited C-atoms from a filament source onto a Ni substrate and generated graphitic carbon by annealing at 800–900 °C.<sup>15</sup> Carbon deposition directly onto SiC (Refs. 16 and 17) and Si (Ref. 18) substrates to form graphitic films has also been investigated by other groups. We have developed a procedure for the MBE-based formation of graphitic carbon on GaAs(100) substrates by *in situ* thermal sublimation of C-doped GaAs (GaAs:C). Controlled layer-by-layer thermal etching of GaAs has been previously reported<sup>19,20</sup> to the extent that it is possible to observe reflection high energy electron diffraction (RHEED) intensity oscillations corresponding to the removal of successive monolayers of GaAs.<sup>21</sup> Importantly, nonvolatile dopant atoms remain on the surface after thermal etching of GaAs.<sup>22</sup> This enables us to use the thermal sublimation of bulk GaAs:C layers to form carbon films on GaAs substrates (Fig. 1). When GaAs:C [Fig. 1(a)] is thermally etched under an  $As_2$  overpressure (to prevent Ga droplet formation), the carbon atoms remain on the surface [Figs. 1(b) and 1(c)]. The total number of carbon atoms in-

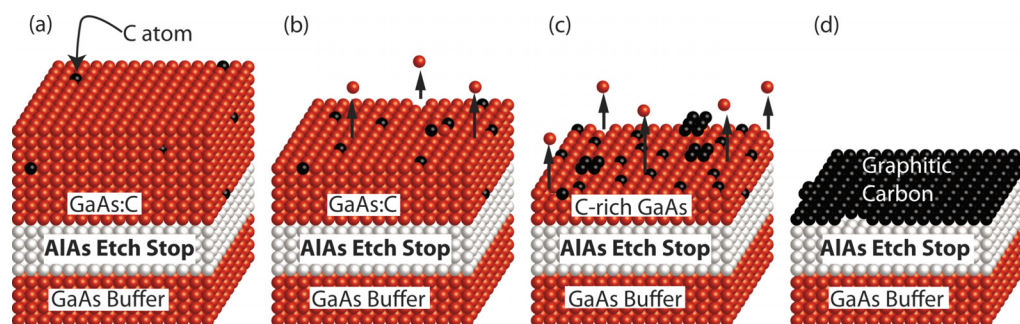


FIG. 1. (Color online) Schematic diagrams depicting the process of MBE-based graphitic carbon synthesis on GaAs. (a) GaAs:C is grown above an AlAs etch stop layer on a GaAs (100) substrate. (b) Under an overpressure of  $As_2$ , substrate temperature is raised such that GaAs etches away in a layer-by-layer fashion. (c) The lower vapor pressure of C-atoms causes them to remain on the surface, and the GaAs surface becomes increasingly carbon-rich. (d) Epitaxially flat AlAs acts as a thermal etch stop layer once all GaAs:C is removed, and a thin layer of C-atoms is left on the surface.

<sup>a)</sup>Electronic mail: jsimon@alumni.nd.edu.

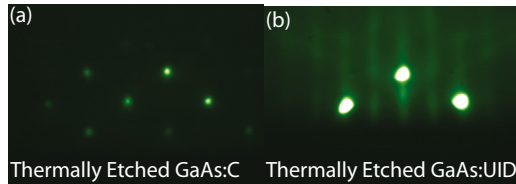


FIG. 2. (Color online) RHEED reconstruction patterns along [011] after thermal etching of (a) GaAs:C and (b) GaAs:UID. The presence of carbon in the films affects the thermal etching process and results in a spotty reconstruction pattern.

incorporated in the GaAs bulk layer determines the number of graphene layers that can be formed. This gives us two degrees of freedom in order to obtain the  $3.8 \times 10^{15} \text{ cm}^{-2}$  carbon atoms needed to produce a single layer of graphene. By adjusting the doping density and/or the C-doped film thickness, we modify the total number of carbon atoms and in turn the number of graphene layers formed after complete etching of the GaAs:C film [Fig. 1(d)].

In order to investigate the formation of graphitic carbon on GaAs, samples were grown in a Veeco GEN-II MBE system on GaAs(100) on axis ( $\pm 0.5^\circ$ ) substrates. Elemental sources of Ga, As<sub>2</sub>, and Al were used, while a CBr<sub>4</sub> source was used to supply the carbon. *In situ* RHEED allowed us to study the surface morphology during growth and subsequent thermal etching of the samples. Two samples were grown with a 5 nm AlAs etch stop layer to provide an atomically flat surface on which the residual carbon can graphitize following the thermal etching of GaAs:C. 2  $\mu\text{m}$  of GaAs:C with  $2 \times 10^{19} \text{ cm}^{-3}$  doping concentration was subsequently grown on top of the AlAs, which contains enough carbon atoms to form a monolayer of graphene. A schematic of the layer structure can be seen in Fig. 1(a). Thermal etching was then carried out under an As overpressure of  $1.6 \times 10^{-5}$  Torr and substrate temperatures ( $T_{\text{SUB}}$ ) of 735 and 800 °C for the two samples. These conditions correspond to thermal etch rates of  $\sim 15$  and 240 nm/min, respectively, calibrated using electron microscopy techniques developed previously.<sup>23,24</sup>

During thermal etching of GaAs:C, RHEED patterns changed from a streaky  $2 \times 4$  reconstruction (not shown) to spotty [Fig. 2(a)]. This spotty RHEED pattern suggests a roughening of the surface of the GaAs:C film. In contrast, RHEED patterns measured during the thermal etching of unintentionally doped GaAs (GaAs:UID) remained streaky [Fig. 2(b)], which suggests that a smooth surface was maintained throughout the etch process. The observed change in the GaAs:C surface reconstruction is an indication that the carbon doping in the films affects the thermal etching process. The surface showed no sign of smoothing as thermal etching proceeded. We speculate that this roughening of the surface during GaAs:C etching is caused by nanoscopic graphitic crystallites forming at the surface of the GaAs:C and masking the subsequent thermal etch of GaAs below them.

To characterize the chemical bonding of the thermally etched GaAs:C surfaces, we performed Raman spectroscopy measurements in a HORIBA LABRAM 300 system, with a 532 nm wavelength incident laser and a  $100\times$  objective lens. A commercially available exfoliated graphene flake on a SiO<sub>2</sub>/Si wafer was used as a Raman reference standard sample. Thermally etched GaAs:C films exhibited vibrational phonon modes at  $\sim 1338$ ,  $\sim 1604$ , and  $\sim 2665 \text{ cm}^{-1}$

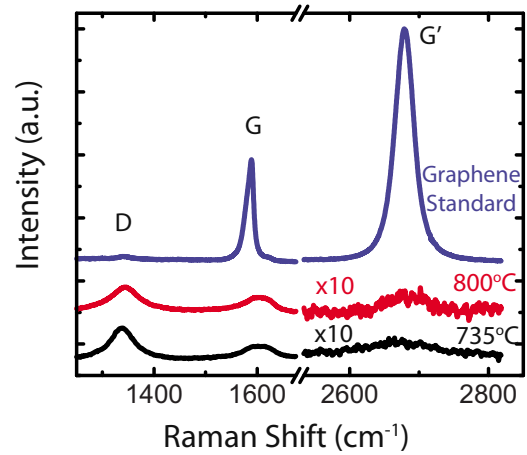


FIG. 3. (Color online) Raman spectra of GaAs:C thermally etched at  $T_{\text{SUB}}=735 \text{ }^\circ\text{C}$  (lower curves) and  $T_{\text{SUB}}=800 \text{ }^\circ\text{C}$  (middle curves) showing characteristic D, G, and G' phonon peaks for  $sp^2$ -bonded carbon. The top curves are from a standard graphene sample and are provided for comparison.

(Fig. 3), which are characteristic of  $sp^2$ -bonded carbon.<sup>25</sup> These three vibrational modes correspond, respectively, to phonons at graphitic zone boundaries (D), the stretching of in-plane carbon-carbon bonds (G), and the second order mode of zone-boundary phonons (G' or 2D).<sup>18,26</sup> These results confirm the presence of graphitic carbon on the surface of the thermally etched GaAs:C.

The large intensity of the D peak as compared to the G phonon peak in our Raman spectrum from the sample etched at 735 °C indicates that the graphitic carbon is highly disordered. Since D mode phonons are associated with edge defects,<sup>26</sup> the relative strength of this peak suggests the presence of numerous graphitic domains rather than a continuous graphene sheet. This is consistent with our theory that small graphitic crystallites form during etching.

When the etch temperature was raised from 735 to 800 °C we observed a 40% reduction (from 2.94 to 1.75) in the ratio of the intensity of the D phonon peak ( $I_D$ ) to the G phonon peak ( $I_G$ ), as seen in Fig. 3. Previous studies have shown that the  $I_D/I_G$  ratio approaches zero for highly ordered graphene sheets.<sup>14,27</sup> Therefore, the reduction of the Raman peak intensity ratio observed in our samples is indicative of a marked improvement in the quality of the graphitic material when etched at higher temperatures. This is most likely caused by an increased surface mobility of the carbon atoms at the higher  $T_{\text{SUB}}$ ; higher  $T_{\text{SUB}}$  is known to increase graphene quality in epitaxial graphene on SiC substrates.<sup>14</sup>

The  $I_D/I_G$  ratio can also be used to estimate the average size ( $L_a$ ) of the graphitic domains on the surface of GaAs (Refs. 27 and 28):

$$L_a = C(\lambda_L) \left( \frac{I_D}{I_G} \right), \quad (1)$$

where  $\lambda_L$  is the wavelength of the excitation light and  $C(\lambda_L)$  is the Raman coupling coefficient given by

$$C(\lambda_L) = C_0 + \lambda_L C_1. \quad (2)$$

The two fitting parameters  $C_0$  and  $C_1$  were obtained experimentally by Matthews *et al.*<sup>29</sup> to be  $-126 \text{ \AA}$  and 0.033, respectively. This results in average graphitic domain sizes

of 1.7 and 2.9 nm for samples thermally etched at  $T_{\text{SUB}}=735$  and  $800$  °C, respectively. The size of our graphitic crystallites is comparable to those previously reported for the graphitization of Si(111) substrates.<sup>18</sup> The formation of larger graphene domains on GaAs substrates will require further optimization of our process in the future by using higher etch temperatures and/or directly depositing C-atoms on AlAs to avoid etch roughness caused by micromasking of the GaAs by the graphitic flakes.

We have demonstrated a method for obtaining graphitized carbon on GaAs(100) surfaces. The *in situ* thermal etching of GaAs:C grown by MBE resulted in the carbon atoms remaining on the surface due to their low vapor pressure. The total number of carbon atoms available is precisely controllable by the doping density and thickness of the GaAs:C layer. Characteristic phonon modes in Raman spectra from the thermally etched surfaces confirm that the residual surface carbon atoms form  $sp^2$ -bonded graphitic crystallites, 1.5–3 nm in size. By raising the thermal etch temperature we demonstrate that crystallite domain size can be increased.

Two of the authors (J.S. and P.J.S.) contributed equally to this work.

- <sup>1</sup>K. I. Bolotin, K. J. Sikes, Z. Jiang, M. Klima, G. Fudenberg, J. Hone, P. Kim, and H. L. Stormer, *Solid State Commun.* **146**, 351 (2008).
- <sup>2</sup>K. S. Novoselov, A. K. Geim, S. V. Morozov, D. Jiang, M. I. Katsnelson, I. V. Grigorieva, S. V. Dubonos, and A. A. Firsov, *Nature (London)* **438**, 197 (2005).
- <sup>3</sup>Y. Zhang, T. T. Tang, C. Girit, Z. Hao, M. C. Martin, A. Zettl, M. F. Crommie, Y. R. Shen, and F. Wang, *Nature (London)* **459**, 820 (2009).
- <sup>4</sup>B. Huang, Q. Yan, G. Zhou, J. Wu, B.-L. Gu, W. Duan, and F. Liu, *Appl. Phys. Lett.* **91**, 253122 (2007).
- <sup>5</sup>Q. Zhang, T. Fang, H. Xing, A. Seabaugh, and D. Jena, *IEEE Electron Device Lett.* **29**, 1344 (2008).
- <sup>6</sup>R. Murali, K. Brenner, Y. Yang, T. Beck, and J. D. Meindl, *IEEE Electron Device Lett.* **30**, 611 (2009).
- <sup>7</sup>S. Bae, H. Kim, Y. Lee, X. Xu, J.-S. Park, Y. Zheng, J. Balakrishnan, T. Lei, H. R. Kim, Y. I. Song, Y.-J. Kim, K. S. Kim, B. Ozyilmaz, J.-H. Ahn, B. H. Hong, and S. Iijima, *Nat. Nanotechnol.* **5**, 574 (2010).
- <sup>8</sup>A. Reina, X. Jia, J. Ho, D. Nezich, H. Son, V. Bulovic, M. S. Dresselhaus, and J. Kong, *Nano Lett.* **9**, 30 (2009).

- <sup>9</sup>K. S. Kim, Y. Zhao, H. Jang, S. Y. Lee, J. M. Kim, K. S. Kim, J.-H. Ahn, P. Kim, J.-Y. Choi, and B. H. Hong, *Nature (London)* **457**, 706 (2009).
- <sup>10</sup>C. Berger, Z. Song, X. Li, X. Wu, N. Brown, C. Naud, D. Mayou, T. Li, J. Hass, A. N. Marchenkov, E. H. Conrad, P. N. First, and W. A. de Heer, *Science* **312**, 1191 (2006).
- <sup>11</sup>E. Rollings, G.-H. Gweon, S. Y. Zhou, B. S. Mun, J. L. McChesney, B. S. Hussain, A. V. Fedorov, P. N. First, W. A. de Heer, and A. Lanzara, *J. Phys. Chem. Solids* **67**, 2172 (2006).
- <sup>12</sup>C. Dimitrakopoulos, Y.-M. Lin, A. Grill, D. B. Farmer, M. Freitag, Y. Sun, S.-J. Han, Z. Chen, K. A. Jenkins, Y. Zhu, Z. Liu, T. J. McArdle, J. A. Ott, R. Wisniewski, and P. Avouris, *J. Vac. Sci. Technol. B* **28**, 985 (2010).
- <sup>13</sup>J. S. Moon, D. Curtis, S. Bui, M. Hu, D. K. Gaskill, J. L. Tedesco, P. Asbeck, G. G. Jernigan, B. L. VanMil, R. L. Myers-Ward, C. R. Eddy, P. M. Campbell, and X. Weng, *IEEE Electron Device Lett.* **31**, 260 (2010).
- <sup>14</sup>J. Robinson, X. Weng, K. Trumbull, R. Cavalero, M. Wetherington, E. Frantz, M. LaBella, Z. Hughes, M. Fanton, and D. Snyder, *ACS Nano* **4**, 153 (2010).
- <sup>15</sup>J. M. Garcia, R. He, M. P. Jiang, J. Yan, A. Pinczuk, Y. M. Zuev, K. S. Kim, P. Kim, K. Baldwin, K. W. West, and L. N. Pfeiffer, *Solid State Commun.* **150**, 809 (2010).
- <sup>16</sup>E. Moreau, F. J. Ferrer, D. Vignaud, S. Godey, and X. Wallart, *Phys. Status Solidi A* **207**, 300 (2010).
- <sup>17</sup>J. Park, W. C. Mitchel, L. Grazulis, H. E. Smith, K. G. Eyink, J. J. Boeckl, D. H. Tomich, S. D. Pauley, and J. E. Hoelscher, *Adv. Mater.* **22**, 4140 (2010).
- <sup>18</sup>J. Hackley, D. Ali, J. DiPasquale, J. D. Demaree, and C. J. K. Richardson, *Appl. Phys. Lett.* **95**, 133114 (2009).
- <sup>19</sup>J. M. Van Hove and P. I. Cohen, *Appl. Phys. Lett.* **47**, 726 (1985).
- <sup>20</sup>W. T. Tsang, T. H. Chiu, and R. M. Kapre, *Appl. Phys. Lett.* **63**, 3500 (1993).
- <sup>21</sup>T. Kojima, N. J. Kawai, T. Nakagawa, K. Ohta, T. Sakamoto, and M. Kawashima, *Appl. Phys. Lett.* **47**, 286 (1985).
- <sup>22</sup>A. C. Warren, J. M. Woodall, E. R. Fossum, G. D. Pettit, P. D. Kirchner, and D. T. McInturff, *Appl. Phys. Lett.* **51**, 1818 (1987).
- <sup>23</sup>R. Fischer, J. Klem, T. J. Drummond, R. E. Thorne, W. Kopp, H. Morko, and A. Y. Cho, *J. Appl. Phys.* **54**, 2508 (1983).
- <sup>24</sup>J.-P. Reithmaier, R. F. Broom, and H. P. Meier, *Appl. Phys. Lett.* **61**, 1222 (1992).
- <sup>25</sup>R. P. Vidano, D. B. Fischbach, L. J. Willis, and T. M. Loehr, *Solid State Commun.* **39**, 341 (1981).
- <sup>26</sup>A. C. Ferrari, J. C. Meyer, V. Scardaci, C. Casiraghi, M. Lazzeri, F. Mauri, S. Piscanec, D. Jiang, K. S. Novoselov, S. Roth, and A. K. Geim, *Phys. Rev. Lett.* **97**, 187401 (2006).
- <sup>27</sup>F. Tuinstra and J. L. Koenig, *J. Chem. Phys.* **53**, 1126 (1970).
- <sup>28</sup>A. C. Ferrari and J. Robertson, *Phys. Rev. B* **61**, 14095 (2000).
- <sup>29</sup>M. J. Matthews, M. A. Pimenta, G. Dresselhaus, M. S. Dresselhaus, and M. Endo, *Phys. Rev. B* **59**, R6585 (1999).